Effects of Solvent Viscosity on Conformational Dynamics of Heme-pocket in Myoglobin and Hemoglobin

Seongheun Kim and Manho Lim*

Department of Chemistry and Chemistry Institute for Functional Materials, Pusan National University, Busan 609-735, Korea
**E-mail: mhlim@pusan.ac.kr*
Received June 28, 2006

The influence of solvent viscosity on conformational dynamics of the heme-pocket, a small vacant site near the binding site of myoglobin (Mb) and hemoglobin (IIb), and playing a functionally important role by serving as a station in ligand binding and escape, was studied by probing time-resolved vibrational spectra of CO photodissociated from MbCO and IIbCO in D_2O, 75 wt% glycerol/D_2O, and trehalose at 283 K. Two absorption bands (B_1 and B_2) of the sample in viscous solvents, arising from CO in the heme pocket, are very similar to those in D_2O. Two bands in Mb and IIb under all three solvents exhibit very similar nonexponential spectral evolution (B_1 band; blue shifting and broadening, B_2 band; narrowing with a negligible shifting), suggesting that in the present experimental time window of 100 ps, the extents of the spectral shift and narrowing is much influenced neither by the viscosity of solvent nor by the quaternary contact of IIb. Spectral evolution can be described by a biexponential function with a fast universal time constant of 0.52 ps and a slow time constant ranging from 13 to 32 ps. For both proteins in all three solvents majority of spectral evolution occurs with the fast universal time constant. The magnitude of the slow rate in the spectral shift of B_1 band decreases with increasing solvent viscosity, indicating that it is influenced by global conformational change which is retarded in viscous solvent, thereby serve as a reporter of global conformational change of heme proteins after deligation.

Key Words : Conformational dynamics, Heme proteins, Heme pocket, Time-resolved IR spectroscopy, Trehalose

Introduction

Protein structural dynamics plays a significant role in the control of protein reactivity and thus its function. Protein undergoes a broad range of structural fluctuation including a large-amplitude collective global motion as well as a smaller and more local internal motion. How global motion of a protein is coupled to functionally important internal motions of the protein is essential to understand biomechanics of protein.[1,2] Coupling between global motion of protein and its internal motion has been studied by influencing protein surface motions using viscous solvent and monitoring the alteration in protein dynamics.[3-5]

Myoglobin (Mb) and hemoglobin (Hb) have been extensively studied as a model system for the experimental and theoretical study of the functional role of protein-solvent interaction as well as protein dynamics and its relation to structure and function.[2,3,6-15] Myoglobin is a monomeric protein that contains a heme prosthetic group and Hb is a tetrameric protein, each monomeric subunit contains a single heme group.[16-18] Several peptides in the vicinity of the heme are highly conserved in various mammalian species. These highly conserved residues encompass a small vacant site near the active binding site, called heme pocket. Heme pocket has been suggested to serve as a station in mediating the passage of ligands to and from the active binding site, thereby modulating ligand-binding activity.[19-21] Understanding structural dynamics of the heme pocket and its coupling to global motion of the protein is essential to unveil its functional role and the mechanism of how the heme pocket mediates ligand transport.

Ultrafast dissociation of CO from MbCO and HbCO generates deligated heme proteins in the CO-ligated conformation and initiates a change in the tertiary conformation of the protein that eventually leads to the quaternary conformational change in Hb. Conformational change of a protein depends on a variety of environmental elements including solvent viscosity. Glycerol has been extensively employed as a viscogenic cosolvent to vary solvent viscosity[22,23] and a glass-forming dried trehalose as an effectively infinite viscosity solvent.[4,5,23,24] Trehalose is a disaccharide with a high glass transition.[25,26] Its solutions are known to form glasses[4,5,23,24] when dried under appropriate condition at biological temperatures.[25] The trehalose glass matrix locks the surface of protein, selectively eliminating the large amplitude solvent-coupled relaxation modes and leaving only side-chain motions and local relaxation modes.[7,24] Conformational relaxation of the protein are severely inhibited in trehalose glass.[4,5,24] Motions at the protein surface would be expected to be quite sensitive to solution properties, whereas local dynamics of the protein interior are influenced by viscosity only to the extent that they are coupled to more global dynamics.

Recently we have shown that conformational dynamics of heme pocket can be probed by time-resolved vibrational spectra of CO photodissociated from MbCO and HbCO in

D_2O.[27] We have found that the spectral evolution is induced by protein conformational changes that modify structure and electric field of heme pocket, and ligand dynamics in it.[27] Here, we have extended our early investigation and study the conformational dynamics of heme pocket in viscous solvents to elucidate how protein surface motion influences the functionally-important internal structural dynamics of the protein.

Materials and Methods

Samples in D_2O solution and 75 wt% glycerol/D_2O were prepared by dissolving 10 mM lyophilized skeletal horse Mb (Sigma) in corresponding solvent buffered with 0.1 M potassium phosphate (pD 7.4). The solution was equilibrated with 1 atm of ^{13}CO (Aldrich, 99.3% ^{13}C, < 1.8% ^{18}O) and reduced with *ca* 2 equivalent concentration of freshly prepared sodium dithionate (Aldrich). The reduced Mb was stirred under 1 atm ^{13}CO for at least 0.5 hour. To remove light scattering sources such as dust particles and denatured protein aggregates, samples were filtered through a 5-μm membrane filter before loading in a gas-tight 50-μm-pathlength sample cell with CaF_2 windows. The trehalose sample was prepared by combining equal amounts of a 10 mM Mb^{13}CO with a 1.5 M trehalose solution. Both solutions were prepared in D_2O buffered with 0.1 M potassium phosphate. A 0.2 mL aliquot of the resulting solution was layered on a CaF_2 window and dried for *ca.* 4 h under a CO atmosphere in a desiccator. The sample was then sealed by applying vacuum grease to the circumference of the window and pushing another CaF_2 window against the first one. The residual water, estimated from vibrational spectra of trehalose (absorption band at 2936 cm^{-1}) and D_2O (absorption band at 2504 cm^{-1}), was *ca* 1.3 D_2O molecules per trehalose molecule (*ca* 7% by weight). A 2.7 mM Hb^{13}CO (11 mM in heme) was prepared in the same way as the preparation of Mb^{13}CO using lyophilized human Hb (Sigma). During data collection the sample cell was rotated sufficiently fast so that each photolyzing laser pulse illuminated a fresh volume of the sample. The temperature of the rotating sample cell was maintained at 283 ± 1 K. The integrity and concentration of sample was checked throughout experiment using UV-Vis and FT-IR spectroscopy (Bruker, Equinox 55). Because water is a strong IR absorber, the sample was prepared in D_2O using ^{13}CO to isotopically shift interested spectrum into a region with greater IR transmission.

The details of the time-resolved mid-IR spectrometer used here were described elsewhere.[28,29] Briefly, Two identical home-built optical parametric amplifiers (OPA), pumped by a commercial Ti:sapphire amplified pulse, were used to generate a visible pump pulse[30] and a mid-IR probe pulse.[31,32] Pump pulse at 580 nm with 3 μJ of energy was generated by frequency doubling of a signal pulse of one OPA in a type-I, 1-mm-thick BBO crystal.[30] Tunable mid-IR probe pulse with duration of 110 fs (*ca* 1 μJ) was generated by difference frequency mixing of the signal and idler pulse of the other OPA in a 1.5-mm-thick, type-I $AgGaS_2$ crystal. Not to perturb sample with intense mid-IR pulse, only a small portion of the IR pulse is used as a probe. After the sample being photolyzed by the visible pump pulse, its transient mid-IR absorbance was measured with the optically-delayed probe pulse. The polarization of the pump pulse was set at the magic angle (54.7) relative to the probe pulse to recover isotropic absorption spectrum. The broadband transmitted probe pulse was detected with a 64-elements $N_2(l)$-cooled HgCdTe array detector. The array detector was mounted in the focal plane of a 320 mm IR monochromator with a 150 *l*/mm grating, resulting in a spectral resolution of *ca.* 1.4 cm^{-1}/pixel at 2100 cm^{-1}. The signal from each of the detector element was amplified with a home-built 64-channel amplifier and digitized by a 12-bit ADC. Chopping the pump pulse at half the repetition frequency of the laser and computing the difference between the pumped and unpumped absorbance determine the pump-induced change in the absorbance of the sample ΔA. Due to the excellent short-term stability of the IR light source (< 0.5% rms), less than 1 × 10^{-4} rms in absorbance units after 0.5 sec of signal averaging was routinely obtained without single shot referencing with an independent detector. The pump spot was made larger than the probe spot to ensure spatially uniform photoexcitation across the spatial dimensions of the probe pulse.[33] The time resolution attained in this work, determined by transient absorption of Si wafer, was < 180 fs full width at half maximum (FWHM).

Results and Discussion

Time-resolved vibrational spectra after photolysis of Mb^{13}CO and Hb^{13}CO in trehalose at 283 K are shown in Figure 1. Time-resolved spectra of the sample in 75 wt% glycerol/D_2O mixture are very similar to those in trehalose (data not shown). These spectra are also very similar to those in D_2O.[27] Absorption features arise from ^{13}CO photodissociated from the heme and residing inside the protein. The spectral region of ^{13}CO photodissociated from Mb^{13}CO and Hb^{13}CO is free from any protein and trehalose absorption but is located in the tail of a strong O-D stretching mode of D_2O at 2504 cm^{-1} with ~300 cm^{-1} FWHM (ε_{max} = 71.5 M^{-1} cm^{-1}).[34] Even a slight spectral shift and/or variation in the width of the O-D absorption band can cause a significant baseline shift in ΔA. As shown in Figure 2, there is a rapidly decaying featureless baseline which is apparent at the lower energy side of two main bands (see Figure 1). While the rapid decay of the baseline in trehalose can be described by a single exponential function with a time constant of 0.12 ± 0.02 ps, that in D_2O by a biexponential function, 0.88 ± 0.02 exp (−t/0.12 ± 0.02 ps) + 0.12 ± 0.02 exp (−t/3.6 ± 0.5 ps). Instrument response function, obtained by differentiating the transient absorption of Si wafer, is well overlapped with the baseline decay of MbCO and HbCO in trehalose (the inset of Figure 2). The rapidly decaying absorption occurs only during the overlap of pump and probe pulses. Sum in the photon energy of 580 nm pump and 2000 cm^{-1} probe is resonant with a strong Q band near 540 nm with 30 nm

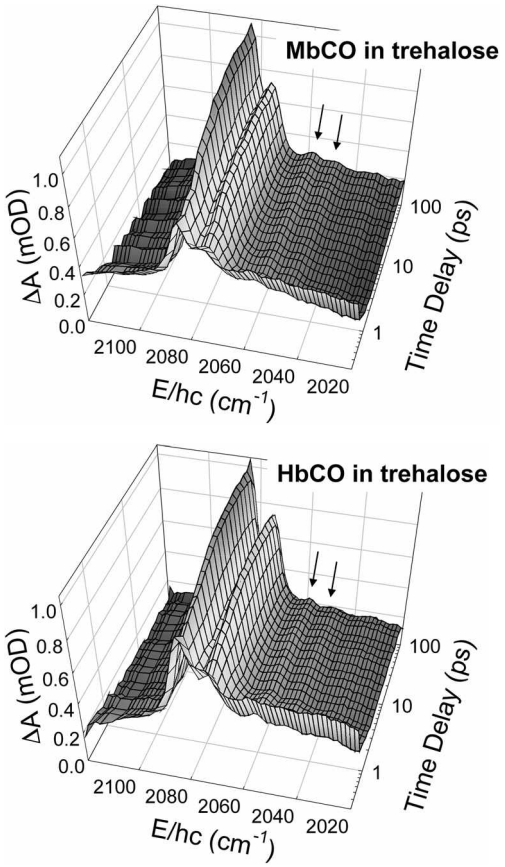

Figure 1. Time-resolved vibrational spectra of ^{13}CO after photodissociation of Mb^{13}CO and Hb^{13}CO in trehalose at 283 K. Small bands near 2050 cm^{-1} (indicated by arrows) arise from vibrationally excited CO (hot band).

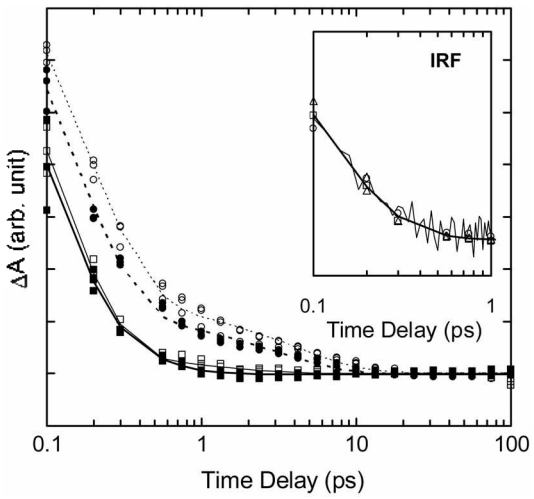

Figure 2. Representative baseline absorbance changes of Hb^{13}CO (open symbols, thin lines) and Mb^{13}CO (filled symbols, thick lines) in trehalose (rectangles, solid lines) and D_2O (circles, dotted lines). Lines are exponential fit (solid lines; single exponential, dotted; biexponential) to the corresponding data. Baseline change was sampled at 2060, 2044, 2022 cm^{-1} and these three points are fit with one exponential function simultaneously. Instrument response function (IRF, thin solid line), obtained by differentiating the transient absorption of Si wafer, is well overlapped with signals of HbCO in trehalose (inset).

FWHM in the heme group. Clearly, the rapidly decaying featureless baseline arises from sum of two photon (pump and probe photons) absorption by the Q band. The slower decaying (3.6 ps component) featureless baseline absorbance, only appearing in the signals of the sample in D_2O, results from absorbance change induced by heating of the solvent.[34-39] The time scale is consistent with transfer time of thermal energy from the chromophore to the solvent.[36-39]

Featureless baseline shift, arising from two photon absorption and absorbance change of solvent by thermal relaxation of the photoexcited protein, was modeled by a cubic polynomial and subtracted for clarity.[19,21] The remaining distinctive features consist of two main bands near 2080 cm^{-1} and two small (~8% of the main band, indicated by arrows in Figure 1) bands near 2050 cm^{-1}. The small band is a red-shifted replica of the main band and has been attributed to absorption of vibrationally excited CO.[19,27] Vibrationally excited CO after photolysis of heme proteins has been found to relax with a time constant of 600 ps and its dynamics is well established.[40] In this article, since we are mainly

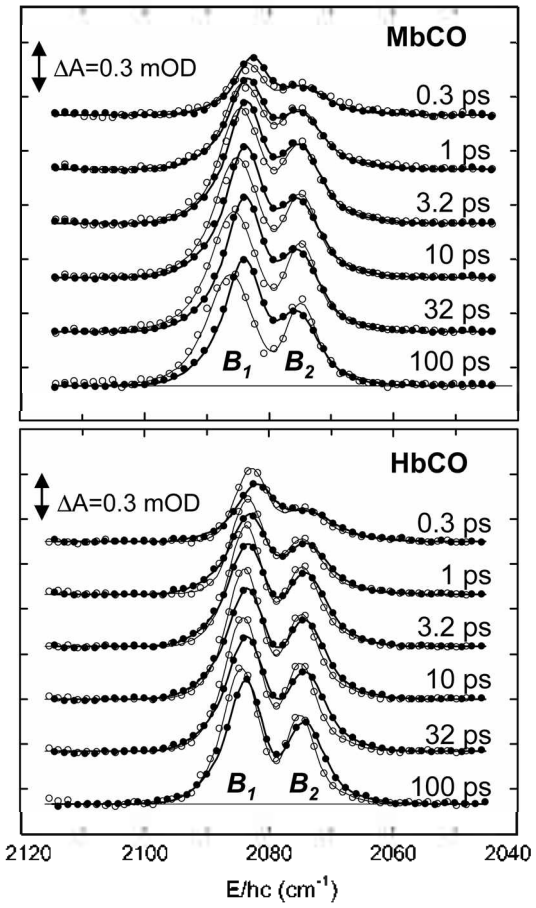

Figure 3. Representative time-resolved vibrational spectra of ^{13}CO photodissociated from Mb^{13}CO and Hb^{13}CO in D_2O (open circles) and trehalose (filled circles) at 283 K. The data (symbols) are fit to two evolving bands (B_1 and B_2) and each band is modeled with a sum of two Gaussians (solid lines). For clarity, the cubic polynomial baseline and a small hot band have been subtracted from the measured spectra. Spectra have been offset one another to avoid overlap.

concerned with the spectral evolution of the main band, the small hot bands are subtracted hereafter. Figure 3 shows the spectral evolution of the two main bands arising from stretching mode of CO photolyzed from MbCO and HbCO in D_2O and trehalose at representative times. Two bands correspond to unbound CO located in the primary docking site with opposite orientations after photolysis from the proteins.[19,21,27,41-43] The spectral evolution in trehalose and 75 wt% glycerol/D_2O mixture are very similar to those in D_2O.[27] Rapid establishment of two bands is consistent with ultrafast photodissociation of Fe-CO in heme proteins[44,45] and the suggestion that CO is funneled into a heme pocket docking site near the binding site after photolysis.[21,42] Clearly, these early dynamics of CO photodissociated from heme proteins are not influenced by the solvent at all.

To characterize the spectral evolution, absorption features were fit to two evolving bands (B_1 and B_2),[19,42] and each band is modeled with a sum of two Gaussians. The sum of two Gaussians depicts an asymmetric band, which likely arises from an anisotropic spatial distribution of photolyzed CO and/or conformational substates of protein.[19,27,42] To recover robust spectral parameters characterizing B-states, the same strategy in global fit of the whole spectra was used as that in the fit of the spectra in D_2O in our previous report.[27] Namely, in each band, the parameters for the small Gaussian were slaved to the main Gaussian by a shift for center wavenumber, a scale factor for standard deviation, and another scale factor for integrated absorbance. Whole spectra of each sample were globally fit using these three-shared parameters and parameters characterizing an evolving Gaussian for each band. Quality of fitting the spectra is excellent (see Figure 3) and recovered parameters are well behaved. To characterize the asymmetric band, the moments rather than center wavenumber and standard deviation of each Gaussian were calculated. The zeroth, the first, and the second moments of a band, M_0, M_1, and M_2 are written by:

$$M_0 = \int \Delta A(\bar{\nu}) d\bar{\nu}$$

$$M_1 = \frac{\int \bar{\nu} \Delta A(\bar{\nu}) d\bar{\nu}}{M_0}$$

$$M_2 = \frac{\int (\bar{\nu} - M_1)^2 \Delta A(\bar{\nu}) d\bar{\nu}}{M_0}$$

where $\bar{\nu}$ is the wavenumber in cm^{-1} unit. The zeroth moment corresponds to the integrated area of the asymmetric absorption band, the first moment is the center of gravity of the band (median wavenumber), and the second moment represents variance of the band (bandwidth). The first and the second moments of each band of the sample in various solvents were analytically calculated from the parameters of two Gaussians and are plotted in Figure 4. In all samples studied here B_2 band narrows significantly at negligibly shifting position, and B_1 band shifts toward higher energy and broadens.[42] The trend of the overall time evolution of B_1 band and B_2 band in 75 wt% glycerol/D_2O and a trehalose appears to be very similar to that in D_2O.[27]

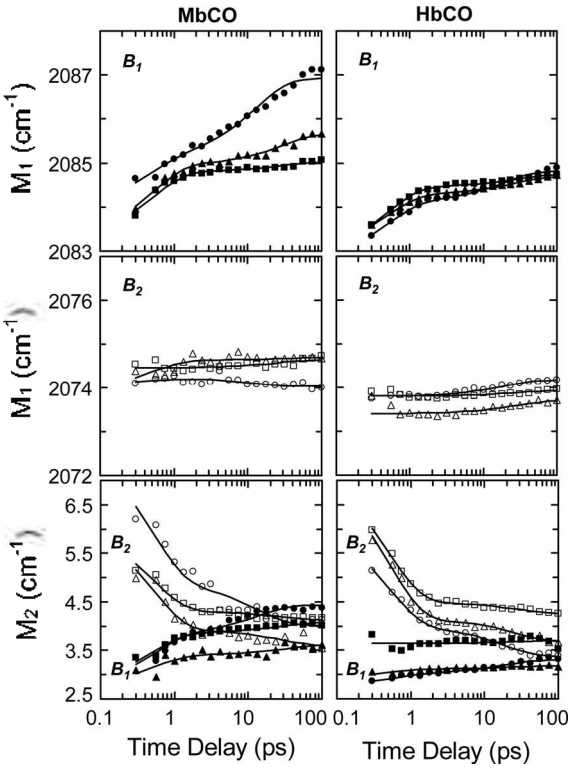

Figure 4. Time evolution of the moments describing bands B_1 (filled symbols) and B_2 (open symbols) for $Mb^{13}CO$ (left panels) and $Hb^{13}CO$ (right panels) in D_2O (circles), 75 wt% glycerol/D_2O (triangles), and trehalose (squares). The moments, M_1 and M_2 are related to median wavenumber and spectral width of absorption band, respectively. The data (symbols) are well described by biexponential functions (solid lines).

However, at a closer look, one can find that spectral shift of B_1 have an obvious and systematic solvent dependence.

The total integrated area of the two main bands (sum of the zeroth moments of the two bands) grows exponentially with a time constant of 1.1 ± 0.1 ps and is maintained a constant magnitude thereafter throughout present experimental window of 100 ps.[21] As shown in Figure 5, the initial growth is the same for both Mb and Hb and independent of the solvent surrounding heme protein. The initial growth of the integrated area has been attributed to protein arrangement constraining the orientation of the docked CO after photolysis.[21] Clearly, the time scale for the rearrangement is not influenced by the solvent viscosity, suggesting that protein motions involved in the rearrangement are negligibly coupled to the solvent. It has been found that only small amplitude side-chain motions isolated from the solvent in the interior of the protein is responsible for protein motions needed to establish the ligand interconversion barrier in the primary docking site.[46] The same category of dynamics is likely involved in the early rearrangement of the residues surrounding heme pocket. The persistent magnitude of the total integrated area after the initial growth is consistent with the idea that escape of CO from the heme pocket and geminate rebinding of CO to Mb and Hb are much slower than 100 ps in all the samples investigated here.[47] The

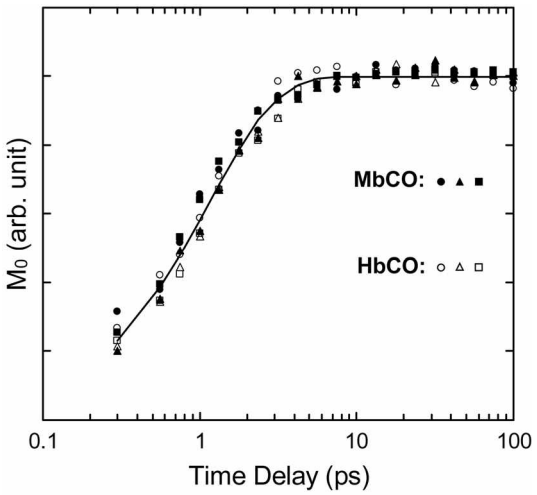

Figure 5. Total integrated absorbance changes of ^{13}CO photodissociated from Mb^{13}CO (filled symbols) and Hb^{13}CO (open symbols) in D_2O (circles), 75 wt% glycerol/D_2O (triangles), and trehalose (squares). The time-dependent integrated absorbance is well reproduced by an exponential function of the form $(1 - \exp(-t/\tau_{rise}))$ with $\tau_{rise} = 1.1 \pm 0.1$ ps (solid line).

similarity of the growth time of the integrated area of Mb and Hb suggests that the quaternary structure of Hb has a negligible influence on the early protein rearrangement influencing ligand motion in the primary docking site (*B* site) after photolysis. It also indicates that the dynamics of ligand in the primary docking site is well preserved in Mb and Hb.

In our previous study of conformational dynamics of heme pocket in Mb and Hb in D_2O,[27] we found that B_1 band shifts toward higher energy and broadens and B_2 band barely shifts but narrows significantly. The behavior of the B_1 band has been attributed to the variation of the electric field at B_1 site induced by protein conformational relaxation after photolysis[21,27,48] and that of the B_2 band to tightening of the heme pocket arising from conformational relaxation.[27] We also found that the overall spectral shift of B_1 in Hb is smaller than that of Mb, suggesting that the spectral shift of B_1 is strongly influenced by conformational relaxation of the protein after photolysis and it is a good reporter for the conformational relaxation influencing ligand dynamics in heme pocket.[27]

As has been observed in our previous experiment, a biexponential function well describes time evolution for the first and the second moments of B_1 and B_2 bands of CO photolyzed from MbCO and HbCO under different viscosity environments. Time evolution for both moments of the two bands in three different solvents, obtained by global fitting of each complete set of spectra, was modeled by biexponential functions:

$$\Delta M_i^j(t) = a_{f,i}^j \exp(-t/\tau_f) + a_{s,i}^j \exp(-t/\tau_s),$$
$$i = 1, 2 \text{ and } j = B_1, B_2$$

where ΔM_1 and ΔM_2 are the extent of the spectral shift and change in the spectral width of each band. Shared time constants (τ_f and τ_s) and corresponding amplitudes are recovered from the fit. Because the spectral evolution results from the same structural origin, the rates for both moments of the two bands of CO in the heme pocket are likely the same for a given sample. Thus time constants of the biexponential functions were shared for both moments (M_1 and M_2) of the two bands (B_1 and B_2) for a given sample. The faster time constants from the above fit turned out to be very similar one another and are almost independent of the protein and the solvent. Therefore, in the final fitting of the time evolution of the moments, both moments of the two bands of Mb and Hb in three different solvents were globally fit using a fast global time constant for all the six samples (Mb and Hb in three solvents) and slow six time constants shared for both moments of the two bands of each sample. As can be seen in Figure 4, the global fit well reproduces the time evolution of both moments of the two bands in Mb and Hb under different solvents. The recovered fast global time constant is 0.52 ps and the slow time constants are ranging from 13 to 32 ps. The global time constant of 0.52 ps, appearing Mb and Hb in all three solvents studied here, is universal and likely arises from protein dynamics preserved in heme protein. As has been suggested, the slow rate constants are comparable with the time scale for conformational relaxation of protein after photolysis.[27,49,50]

The spectral evolution due to conformational relaxation is most apparent in the second moment of B_2 band and the first moment of B_1 band. Majority of the spectral narrowing of B_2 band occurs with the fast global time constant of 0.52 ps. For both Mb and Hb in three different solvents, 84 ± 7% of spectral narrowing (out of total spectral narrowing in 100 ps) occurs with the fast global time constant. Clearly the early time spectral narrowing is influenced neither by the solvent viscosity nor by quaternary contact of Hb. For B_2 band, even the slower narrowing does not have any significant solvent dependence. Scatter in the magnitude of spectral narrowing of B_2 is large enough to extract any meaningful solvent-dependent trend. On the other hand, as summerized in Table 1, time evolution of M_1 of B_1 band in 100 ps, $\Delta M_1^{B_1}$ exhibits obvious solvent dependence in the slow component. The slow rate for $\Delta M_1^{B_1}$ shows the tendency of being slowed with increasing solvent viscosity. In particular, the magnitude of the slow component of $\Delta M_1^{B_1}$, $a_{s,1}^{B_1}$ decreases

Table 1. The fitted parameters of ΔM_1 for B_1 band of MbCO and HbCO at various solvents. ΔM_1 for B_1 band in all three solvents are globally fit to a biexponential function of the form $a_{f,1}^{B_1} \exp(-t/\tau_f) + a_{s,1}^{B_1} \exp(-t/\tau_s)$ with a shared time constant, τ_f

sample	solvent	τ_f (ps)	τ_s (ps)	$a_{f,1}^{B_1}$	$a_{s,1}^{B_1}$
MbCO	D_2O	0.52	13	1.03	1.81
	75 wt% G/W		32	1.70	0.73
	trehalose		28	1.58	0.21
HbCO	D_2O	0.52	19	1.33	0.71
	75 wt% G/W		29	1.28	0.41
	trehalose		29	1.53	0.29

significantly as solvent becomes more viscous, suggesting that $a_{s,1}^{B_1}$ reflects the extent of conformational relaxation of the protein after deligation. Since conformational relaxation of protein in viscous medium is retarded, as solvent becomes more viscous, the magnitude of conformational relaxation in viscous solvent in 100 ps after deligation will be smaller. Since the quaternary contact in Hb slows conformational relaxation, too, the extent of the relaxation will be smaller than that in Mb in a given time. Interestingly, the magnitude of $a_{s,1}^{B_1}$ in Hb is smaller than that in Mb under corresponding solvent, corroborating that it is indeed a marker for the conformational relaxation of heme protein after deligation. One exception is that the magnitude of $a_{s,1}^{B_1}$ in Hb in trehalose is similar to that in Mb, suggesting that the retardation in conformational relaxation of heme protein by trehalose glass is larger than that imposed by the quaternary contact of Hb. While the slow component of $\Delta M_1^{B_1}$ can serve as a maker for conformational relaxation of heme protein after deligation, the fast component in $\Delta M_1^{B_1}$ is dominating the whole shift and the magnitude of the shift ($a_{f,1}^{B_1}$), 1.4 ± 0.4 cm^{-1} in 100 ps, appears to be the same for all the samples shown here. This observation also suggests that the fast spectral evolution with the universal time constant arises from local dynamics of protein interior poorly coupled with global protein dynamics and is an intrinsic protein dynamics well preserved in heme protein.

In conclusion, we have measured the spectral evolution of the absorption band of CO photodissociated from MbCO and HbCO in different viscosity solvents at 283 K using time-resolved vibrational spectroscopy. The time evolution of the moments characterizing the spectral evolution of the absorption is well described by a biexponential function. We have found that the time evolution of the moments of CO absorption bands has a fast global time constant of 0.52 ps that is influenced neither by the quaternary contact of Hb nor viscosity of solvent. The magnitude of the slow spectral shift of B_1 band decreases as viscosity of solvent increases, suggesting that it can serve as a reporter for the extent of conformational relaxation of heme protein after deligation. The fast global time constant is likely related to local dynamics of protein interior that is not influenced by solvent viscosity.[5,7,50] We suggest that the fast spectral evolution results from a rapid local relaxation of heme protein coupled with the rearrangement of adjacent side chains without being influenced by solvent viscosity, and slow spectral evolution of B_1 is sensitive to a slower global relaxation of the proteins coupled of surface motion of protein.

Acknowledgement. This work was supported for two years by Pusan National University Research Grant. We thank Mr. Jeonghee Heo for help in preparation of the samples. We are grateful to the Central Laboratory at Pusan National University for our unrestricted access to the femtosecond laser system.

References

1. Ansari, A.; Berendzen, J.; Braunstein, D. K.; Cowen, B. R.; Frauenfelder, H.; Hong, M. K.; Iben, I. E. T.; Johnson, J. B.; Ormos, P. *et al. Biophys. Chem.* **1987**, *26*, 337-355.
2. Vitkup, D.; Ringel, D.; Petsko, G. A.; Karplus, M. *Nature Struct. Biol.* **2000**, *7*, 34-38.
3. Beece, D.; Eisenstein, L.; Frauenfelder, H.; Good, D.; Marden, M. C.; Reinisch, L.; Reynolds, A. H.; Sorensen, L. B.; Yue, K. T. *Biochem.* **1980**, *19*, 5147-5157.
4. Hagen, S. J.; Hofrichter, J.; Eaton, W. A. *J. Phys. Chem.* **1996**, *100*, 12008-12021.
5. Gottfried, D. S.; Peterson, E. S.; Sheikh, A. G.; Wang, J.; Yang, M.; Friedman, J. M. *J. Phys. Chem.* **1996**, *100*, 12034-12042.
6. Springer, B. A.; Sligar, S. G.; Olson, J. S.; Phillips, G. N., Jr. *Chem. Rev.* **1994**, *94*, 699-714.
7. Dantsker, D.; Samuni, U.; Friedman, J. M.; Agmon, N. *Biochim. Biophys. Acta, Proteins and Proteomics* **2005**, *1749*, 234-251.
8. Quillin, M. L.; Arduini, R. M.; Olson, J. S.; Phillips, G. N., Jr. *J. Mol. Biol.* **1993**, *234*, 140-155.
9. Barrick, D. *Biochem.* **1994**, *33*, 6546-6554.
10. Clore, G. M.; Gronenborn, A. M. *Prog. Nucl. Mag. Res. Spec.* **1991**, *23*, 43-92.
11. Braunstein, D. P.; Chu, K.; Egeberg, K. D.; Frauenfelder, H.; Mourant, J. R.; Nienhaus, G. U.; Ormos, P.; Sligar, S. G.; Springer, B. A.; Young, R. D. *Biophys. J.* **1993**, *65*, 2447-2454.
12. Jackson, T. A.; Lim, M.; Anfinrud, P. A. *Chem. Phys.* **1994**, *180*, 131-140.
13. Janes, S. M.; Dalickas, G. A.; Eaton, W. A.; Hochstrasser, R. M. *Biophys. J.* **1988**, *54*, 545-549.
14. Oldfield, E.; Guo, K.; Augspurger, J. D.; Dykstra, C. E. *J. Am. Chem. Soc.* **1991**, *113*, 7537-7541.
15. Elber, R.; Karplus, M. *Science* **1987**, *235*, 318-321.
16. Perutz, M. F.; Mathews, F. S. *J. Mol. Biol.* **1966**, *21*, 199-202.
17. Takano, T. *J. Mol. Biol.* **1977**, *110*, 569-584.
18. Stryer, L. *Biochemistry*; San Francisco, 1988; Vol. 3.
19. Lim, M.; Jackson, T. A.; Anfinrud, P. A. *J. Chem. Phys.* **1995**, *102*, 4355-4366.
20. Lim, M.; Jackson, T. A.; Anfinrud, P. A. *Science* **1995**, *269*, 962-966.
21. Lim, M.; Jackson, T. A.; Anfinrud, P. A. *Nature Struct. Biol.* **1997**, *4*, 209-214.
22. Ansari, A.; Jones, C. M.; Henry, E. R.; Hofrichter, J.; Eaton, W. A. *Science* **1992**, *256*, 1796-1798.
23. McClain, B. L.; Finkelstein, I. J.; Fayer, M. D. *J. Am. Chem. Soc.* **2004**, *126*, 15702-15710.
24. Librizzi, F.; Viappiani, C.; Abbruzzetti, S.; Cordone, L. *J. Chem. Phys.* **2002**, *116*, 1193-1200.
25. Green, J. L.; Angell, C. A. *J. Phys. Chem.* **1989**, *93*, 2880-2882.
26. Crowe, L. M.; Reid, D. S.; Crowe, J. H. *Biophys. J.* **1996**, *71*, 2087-2093.
27. Kim, S.; Heo, J.; Lim, M. *Bull. Korean Chem. Soc.* **2005**, *26*, 151-156.
28. Kim, S.; Jin, G.; Lim, M. *J. Phys. Chem. B* **2004**, *108*, 20366-20375.
29. Park, J.; Kim, S.; Lim, M. *Bull. Korean Chem. Soc.* **2005**, *26*, 995-997.
30. Lim, M.; Wolford, M. F.; Hamm, P.; Hochstrasser, R. M. *Chem. Phys. Lett.* **1998**, *290*, 355-362.
31. Hamm, P.; Lim, M.; Hochstrasser, R. M. *J. Phys. Chem. B* **1998**, *102*, 6123-6138.
32. Hamm, P.; Kaindl, R. A.; Stenger, J. *Opt. Lett.* **2000**, *25*, 1798-1800.
33. Lim, M. *Bull. Korean Chem. Soc.* **2002**, *23*, 865-871.
34. Venyaminov, S. Y.; Prendergast, F. G. *Anal. Biochem.* **1997**, *248*, 234-245.
35. Lian, T.; Locke, B.; Kholodenko, Y.; Hochstrasser, R. M. *J. Phys. Chem.* **1994**, *98*, 11648-11656.
36. Li, P.; Champion, P. M. *Biophys. J.* **1994**, *66*, 430-436.
37. Lim, M.; Jackson, T. A.; Anfinrud, P. A. *J. Phys. Chem.* **1996**, *100*, 12043-12051.

38. Lingle, R., Jr.; Xu, X.; Zhu, H.; Yu, S. C.; Hopkins, J. B. *J. Phys. Chem.* **1991**, *95*, 9320-9331.
39. Lingle, R., Jr.; Xu, X.; Zhu, H.; Yu, S. C.; Hopkins, J. B.; Straub, K. D. *J. Am. Chem. Soc.* **1991**, *113*, 3992-3994.
40. Sagnella, D. E.; Straub, J. E.; Jackson, T. A.; Lim, M.; Anfinrud, P. A. *Proc. Natl. Acad. Sci. U.S.A.* **1999**, *96*, 14324-14329.
41. Alben, J. O.; Beece, D.; Bowne, S. F.; Doster, W.; Eisenstein, L.; Frauenfelder, H.; Good, D.; McDonald, J. D.; Marden, M. C. *et al. Proc. Nat. Acad. Sci.* **1982**, *79*, 3744-3748.
42. Lim, M.; Jackson, T. A.; Anfinrud, P. A. *J. Am. Chem. Soc.* **2004**, *126*, 7946-7957.
43. Kim, S.; Lim, M. *J. Am. Chem. Soc.* **2005**, *127*, 5786-5787.
44. Anfinrud, P. A.; Han, C.; Hochstrasser, R. M. *Proc. Natl. Acad. Sci. U.S.A.* **1989**, *86*, 8387-8391.
45. Petrich, J. W.; Poyart, C.; Martin, J. L. *Biochem.* **1988**, *27*, 4049-4060.
46. Kim, S.; Heo, J.; Lim, M. *J. Am. Chem. Soc.* **2006**, *128*, 2810-2811.
47. Henry, E. R.; Sommer, J. H.; Hofrichter, J.; Eaton, W. A. *J. Mol. Biol.* **1983**, *166*, 443-451.
48. Anfinrud, P. A.; Lim, M.; Jackson, T. A. *Proc. of SPIE- Internat. Soc. Opt. Eng.* **1994**, *2138*, 107-115.
49. Kuczera, K.; Lambry, J. C.; Martin, J. L.; Karplus, M. *Proc. Natl. Acad. Sci. U.S.A.* **1993**, *90*, 5805-5807.
50. Lim, M.; Jackson, T. A.; Anfinrud, P. A. *Proc. Natl. Acad. Sci. U.S.A.* **1993**, *90*, 5801-5804.